MOEM

Modern Electronic Materials 2023; 9(1): 15–24
DOI 10.3897/j.moem.9.1.104721

Research Article

Synthesis, structure and electromagnetic properties of FeCoCu/C nanocomposites

Dmitriy G. Muratov[1,2], Lev V. Kozhitov[2], Irina V. Zaporotskova[3], Alena V. Popkova[4], Vitaly A. Tarala[5], Evgenij Yu. Korovin[6], Artem V. Zorin[2]

1 A.V. Topchiev Institute of Petrochemical Synthesis of the Russian Academy of Sciences, 29 Leninsky Ave., Moscow 119991, Russian Federation

2 National University of Science and Technology "MISIS", 4-1 Leninsky Ave., Moscow 119049, Russian Federation

3 Volgograd State University, 100 Universitetsky Ave., Volgograd 400062, Russian Federation

4 JSC "Research Institute NPO" LUCH", 24 Zheleznodorozhnaya Str., Podolsk 142103, Russian Federation

5 North Caucasian Federal University, 1 Pushkin Str., Stavropol 355017, Russian Federation

6 Tomsk State University, 36 Lenin Ave., Tomsk 634050, Russian Federation

Corresponding author: Dmitriy G. Muratov (muratovdg@yandex.ru)

Received 4 March 2023 ♦ **Accepted** 11 March 2023 ♦ **Published** 31 March 2023

Citation: Muratov DG, Kozhitov LV, Zaporotskova IV, Popkova AV, Tarala VA, Korovin EYu, Zorin AV (2023) Synthesis, structure and electromagnetic properties of FeCoCu/C nanocomposites. *Modern Electronic Materials* 9(1): 15–24. https://doi.org/10.3897/j.moem.9.1.104721

Abstract

FeCoCu ternary nanoparticles distributed and stabilized in the carbon matrix of FeCoCu/C metal-carbon nanocomposites have been synthesized using controlled IR pyrolysis of precursors consisting of the "polymer / iron acetylacetate / cobalt and copper acetates" type system obtained by joint dissolution of components followed by solvent removal. The effect of the synthesis temperature on the structure, composition and electromagnetic properties of the nanocomposites has been studied. By XRD was shown that the formation of the FeCoCu ternary nanoparticles occurs due to the interaction of Fe3C with the nanoparticles of the CoCu solid solution. An increase in the synthesis temperature leads to an increase in the size of the metal nanoparticles due to their agglomeration and coalescence as a result of matrix reconstruction. Furthermore, ternary alloy nanoparticles having a variable composition may form depending on the synthesis temperature and the content ratio of the metals. Raman spectroscopy has shown that the crystallinity of the carbon matrix of the nanocomposites increases with the synthesis temperature. The frequency responses of the relative permittivity and permeability of the nanocomposites have been studied at 3–13 GHz. It has been shown that a change in the content ratio of the metals noticeably increases both the dielectric and the magnetic losses. The former loss is caused by the formation of a complex nanostructure of the nanocomposite carbon matrix while the latter one originates from an increase in the size of the nanoparticles and a shift of the natural ferromagnetic resonance frequency to the low-frequency region. The reflection loss has been calculated using a standard method from the experimental data on the frequency responses of the relative permittivity and permeability. It has been shown that the frequency range and the absorption of electromagnetic waves (from –20 to –52 dB) can be controlled by varying the content ratio of the metals in the precursor. The nanocomposites obtained as a result of the experiment deliver better results in comparison with FeCo/C nanocomposites synthesized under similar conditions.

Keywords

metal-carbon nanocomposites, relative permittivity and permeability, FeCoCu nanoparticles, Raman spectroscopy, reflection loss, loss tangent

1. Introduction

Magnetic nanoparticles (materials) play an important role in the rapidly developing branches of advanced science and industry. Magnetic nanoparticles show good promise for the development of magnetic storage media and the synthesis of ferromagnetic liquids [1, 2], in medicine for the transport of medication, as contrasting pigments for magnetic resonance tomography, in hyperthermia treatment [3], in chemistry as catalysts of various petrochemical processes [4], and as ternary metallic catalysts consisting of Cu@FeCo nanoparticle cores and shells that provide for cost reduction due to the absence of noble metals and a substantial improvement of the catalytic activity [5].

Magnetic nanocomposites (e.g. magnetic nanoparticles coated with non-magnetic insulating materials) have been since recently used in the production of electromagnetic radiation absorbers. As compared with conventional ferrite-based absorbers, metals and magnetically soft alloys encapsulated in various non-magnetic shells possess all the required parameters: high magnetic moment and susceptibility, low coercive force and high resistivity.

The synthesis of Fe-, Co- and Ni-containing binary magnetic alloy nanoparticles allows varying their magnetic properties over a wide range [6–11]. Fe–Co binary alloys possess unique physical properties: high Curie temperature, high saturation magnetization and relative permeability and low coercitivity which make them preferable to monometallic nanoparticles of iron group metals [12]. The high magnetization level and the low coercitivity combined with the high initial relative permeability of multicomponent alloy nanoparticles provide for their high efficiency as microwave electromagnetic absorbers [13, 14].

The high cost of Co gives impetus to studies of the structure and electromagnetic properties of FeCo nanoparticles in which Co is replaced for another metal (Ni, Al or Cu). According to recent publications [8, 10, 11, 15], the Fe–Ni–Co ternary alloy synthesized using different methods shows good magnetically soft properties (high saturation magnetization and low coercitivity).

Analysis of reported works suggests that the magnetic parameters of multicomponent alloys depend on the chemical composition of the alloy and the size, morphology and crystallinity of the nanoparticles.

We synthesized FeCoNi/C nanocomposite which is but slightly inferior to FeCo/C nanocomposite in electromagnetic radiation absorption [16, 17]. Study of the electrophysical properties of FeCoNi/C nanocomposites showed their high efficiency as fillers for UHF electromagnetic radiation absorbers [18].

The $Fe_xNi_{80-x}Co$ (x = 50) nanocrystalline ternary alloy having a variable composition was synthesized [10] using chemical reduction following which the nanoparticles were coated with polyethylene glycol 200 (PEG 200) for oxidation and nanoparticle adhesion protection. The saturation magnetization of the ternary alloy specimens was in a 41–54 A · m^2/kg range, the coercive force decreasing from 170 to 122 Oe with a decrease in the Fe content.

It is of interest to consider the synthesis and electromagnetic properties of FeCoCu/C nanocomposite.

Cu@FeCo nanoparticles containing Cu cores and FeCo shells were synthesized using chemical reduction [5]. The nanoparticles exhibited a composition-dependent activity to the catalytic hydrolysis of ammonia boron-hydride (NH, BHs.AB). $Cu_{0.3}@Fe_{0.1}Co_{0.6}$ nanoparticles showed the best catalytic activity for which the highest AB hydrogen generation rate could be as high as 6674.2 ml/(min · g) at 298 K. The elevated catalytic activity is mainly accounted for by the synergetic effect of Cu and Co in the core/shell structured nanoparticles [5].

A correlation was found between the phase composition and the magnetic properties of the Cu–Ni–Co–Fe alloys synthesized by crushing alloy components in a ball mill followed by annealing of the crushed product [19]. The good magnetic properties of the nanocrystalline magnetic alloys originate from the uniform distribution and single-domain configuration of the magnetic phase. Ball milling followed by isothermal heat treatment at 350 °C produced a single-phase solid solution of the Cu–Ni–Fe–Co quaternary alloy with an excess of Cu (35–60 wt.%). The best combination of the magnetic properties was obtained for the 60Cu–15Ni–12.5Co–12.5Fe alloy after isothermal heat treatment at 450 °C for 1 h. One should note that the copper content chosen for the FeCoNi alloy matrix [19] reduced the magnetic properties of the ternary alloy (the saturation magnetization became lower than 50 A · m^2/kg).

Thus, there are insufficient literary data on the synthesis of Fe–Co-Cu nanoparticles and the properties of FeCoCu/C nanocomposites.

2. Experimental

The FeCoCu/C nanocomposites were synthesized using the system containing a polymer (polyacrylonitrile (PAN)), metal salts (iron acetylacetonate, cobalt acetate and copper acetate) and a solvent (dimethylformamide). All the metal salts except iron acetylacetonate were in the form of salt hydrates.

The joint solution principle was used for achieving a uniform distribution of the components in the precursor. Drying at $T \leq 70$ °C removed the solvent, while the uniform distribution of the metals in the polymer was retained due to the formation of donor/acceptor complexes with the nitrile groups of the polymer. The solution was dried to solid residue of a constant weight (hereinafter, the precursor).

After that the precursor was subjected to preliminary annealing in air. The process was stepwise, consisting of heating to 150 °C with holding for 15 min and then heating to 220 °C with holding for 15 min. This stage is

required for the initial cross-linking of the polymer and the formation of a rigid and stable structure of the polymer chains for hindering metal diffusion. The preliminary heat treatment is also required for the decomposition of metal salts to oxides.

The next stage was the synthesis of the metal-carbon nanocomposites. IR heating was in the 500 to 700 °C range in an inert atmosphere (ultra-high purity nitrogen). The linear heating rate was 50 °C, the holding time being 5 min. The specimens were then cooled down and crushed in a mortar to a uniform fraction.

The nanocomposites were synthesized in a MILA-5000 IR furnace (ULVAC GmbH, Germany) having halogen lamps with a total power of 4 kW. The maximum intensity of radiation delivered by these lamps is in the 0.8–1.2 mm range which is optimum for the acceleration of the polymer carbonization processes and the decomposition of the metal-organic salts. The lamps are separated from the reaction zone as they are installed outside the quartz reactor.

The structural and phase composition of nanocomposites was determinated by XRD at room temperature on a DIFRAY X-ray diffractometer in CrK_α radiation. The experimental results were compared against the reference data borrowed from the PDF-4 database (International Centre for Diffraction Data, ICDD). The data of X-ray phase analysis were used for calculating the average sizes of the synthesized FeCo and FeCoCu alloy nanoparticles with the Debye–Scherer equations.

Raman spectra were taken with an inVia Raman Microscope (Renishaw plc) Raman spectrometer with 514 nm laser excitation.

The relative permittivity and permeability were measured using a resonance technique with a rectangular multi-mode resonator. The microwave generator and indicator was a E 8363 B vector network analyzer from Agilent Technologies. The measurements were conducted using equipment and methods developed at the Joint Use Center for Radiophysical Measurements, Diagnostics and Parameter Study of Natural and Artificial Materials of the Tomsk State University[1].

The reflection loss was calculated using the following relationships in the assumption that the nanocomposite layer is infinite, planar and positioned on the metal, and that a planar wave is incident from the ambient space.

$$RL = \frac{Z_{in} - 1}{Z_{in} + 1}, \quad (1)$$

where Z_{in} is the input impedance of the ambient space / specimen interface.

$$Z_{in} = iZ\mathrm{tg}(kd), \quad (2)$$

where Z is the wave impedance of the planar layer provided it is positioned on the metal layer, k is the wavenumber, d is the thickness and RL is the reflection loss.

$$Z = \sqrt{\frac{\mu' + \mu''}{\varepsilon' + \varepsilon''}}; \quad (3)$$

$$k = \frac{2\pi f \sqrt{\varepsilon^* \mu^*}}{c}. \quad (4)$$

3. Results and discussion

The introduction of a diamagnetic metal, i.e., copper, into the Fe–Co system changes both the microstructure and the properties of the FeCoCu alloys.

[1] Tomsk Regional Joint Use Center. URL: http://www.ckp.tsu.ru/about/directions/radiophysics

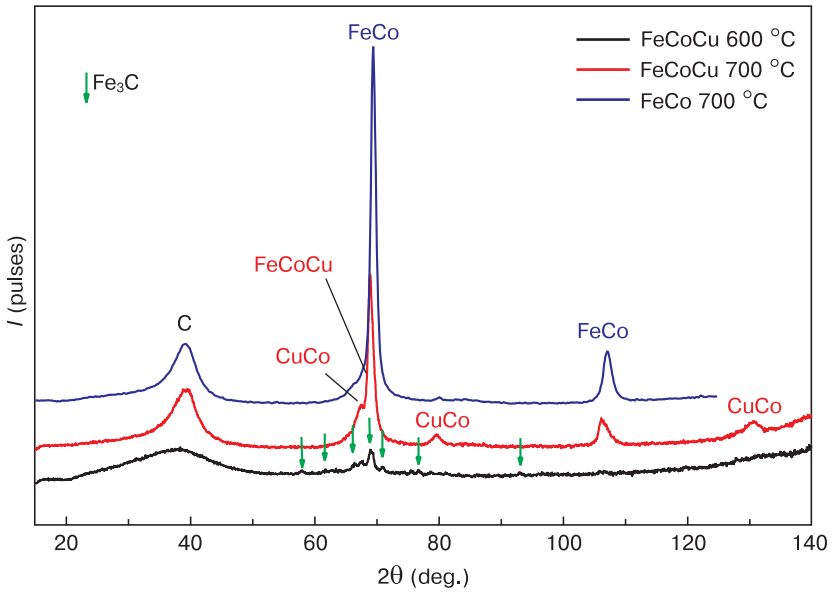

Figure 1. X-ray diffraction patterns of FeCo/C and FeCoCu/C nanocomposites synthesized at different temperatures

X-ray phase analysis showed that, unlike the FeCo/C nanocomposites (with equiatomic metal contents), the PAN-based FeCoCu/C nanocomposites do not form single-phase systems. X-ray diffraction patterns of the FeCoCu/C nanocomposites synthesized at 500–700 °C are shown in Fig. 1 along with those of the FeCo/C nanocomposites synthesized at 700 °C (by way of comparison).

The introduction of copper in the FeCo alloy affects the phase composition and structural patterns of the nanocomposites. It should be taken into account that the solubility of copper in iron is but a few percents whereas its solubility in cobalt is higher. One should also bear in mind that the reduction of copper and cobalt may occur at about 200 °C while the reduction of iron requires 450 °C or higher (depending on the reducing agent).

Phase analysis of the FeCoCu/C nanocomposite specimens synthesized at $T = 600$ °C showed that the metallic phase was present in the synthesized nanocomposites in the form of intermetallides because the X-ray diffraction patterns did not contain reflections corresponding to the copper phase with a face-centered cubic lattice (fcc) or to the pure cobalt phase. The nanocomposites contain three types of nanoparticles: the CuCo solid solution on the basis of cobalt's fcc lattice, the FeCo phase on the basis of iron's body-centered cubic lattice (bcc) and the Fe_3C phase. The intensity of the reflections corresponding to the metal-containing phases is but moderate, suggesting a small size of the nanoparticles.

Comparing phase analysis data for FeCoCu/C with those for the FeCo/C nanocomposites one can find that part of iron is in the form of carbide in the FeCoCu/C nanocomposite synthesized at 600 °C. It seems that the formation of the CuCo alloy reduces the probability of cobalt dissolution in iron.

An increase in the FeCoCu/C nanocomposite synthesis temperature to $T = 700$ °C causes major changes to the phase composition. Comparison of the X-ray diffraction patterns shows the following:

– an increase in the nanocomposite synthesis temperature leads to a tangible increase in the intensity of the reflections corresponding to the metallic phases, suggesting an increase in the particle sizes;

– the Fe_3C reflections are completely eliminated;

– the positions of the bcc phase reflection maxima shift to the low diffraction angles, suggesting an increase in the lattice parameter as a result of iron dissolution.

The iron carbide reflections are eliminated with an increase in the synthesis temperature since the diffusion rate increases at higher temperatures, presumably resulting in the interaction between the nanoparticles having different crystal lattice types (CoCu, FeCo and Fe_3C). The interaction of cobalt and copper with the Fe_3C nanoparticles leads to partial dissolution of these metals. This in turn causes the decomposition of iron carbide and the formation of FeCoCu nanoparticles. A similar observation was made for Cu-Fe/C nanocomposites [20]. The shift of the diffraction maxima is shown in Fig. 2.

Calculation of the coherent scattering region (CSR) sizes for the metal-containing nanoparticles in the FeCoCu/C nanocomposites showed that the average size of the CoCu nanoparticles grows from 6 to 11 nm with an increase in the synthesis temperature from 600 to 700 °C, whereas the size of the bcc phase nanoparticles increases from 8 to 16 nm which is far smaller than that for the FeCo/C nanocomposites without copper (18 nm).

The growth of the nanoparticle sizes with an increase in the synthesis temperature is attributable to metal agglomeration and coalescence during the structural transformation of the nanocomposite carbon matrix and the reduction of iron oxides.

An increase in the relative copper content in the nanocomposites leads to changes in the phase composition and a redistribution of the reflection intensities of the above-mentioned phases (Fig. 3).

The reflection maximum of the bcc phase shift towards the higher angles and corresponds to the FeCo bcc phase, whereas the fcc peaks shift leftwards, indicating the formation of a CuCo solid solution having an almost equiatomic composition. Accordingly, the remainder of copper is present in the form of oxides, probably due to secondary oxidation in air.

Along with changes to the metallic phases, an increase in the synthesis temperature causes changes in the structure of the carbon matrix. The X-ray diffraction of the composite grown at 600 °C (Fig. 1) contains an amorphous halo at 2θ angles of 20° to 45° which are typical of the graphite phase. This shape of the peak is typical of turbostratic carbon the amorphous state of which originates from the small sizes of the coherent scattering regions in the crystallites and an irregular mutual shift of the graphene planes. An increase in the synthesis temperature to 700 °C renders the halo more symmetrical, increases its intensity and forms a maximum corresponding to low-ordered graphite. A Raman scattering study was conducted in order to make an insight into the formation

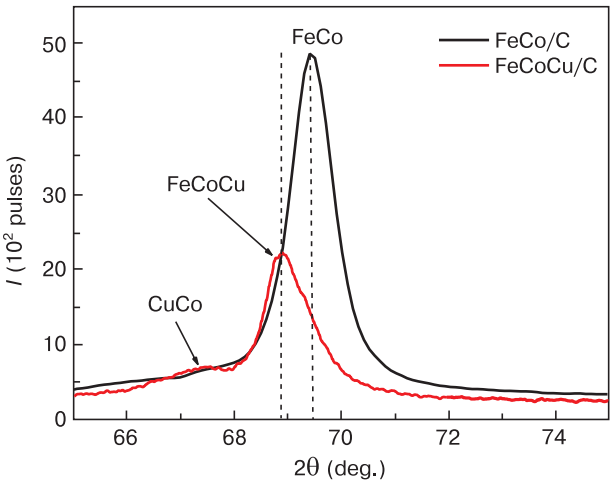

Figure 2. X-ray diffraction patterns of FeCo/C и FeCoCu/C nanocomposites synthesized at 700 °C (2θ = 65–75° angular range)

Table 1. Raman data for FeCoCu/C nanocomposites

$T_{synt.}$ (°C)	Fe : Co : Cu ratio	I_D/I_G	I_{2D}/I_G	$I_{D'}/I_G$	L_a (nm)
500	40 : 40 : 20	1.43	0.35	0.88	3.1
600	40 : 40 : 20	1.17	0.29	0.67	3.8
700	40 : 40 : 20	0.9	0.14	0.61	4.9
700	35 : 35 : 30	0.92	0.15	0.63	4.8

*L_a was calculated using the Tuinstra–Koenig formula [21].

of the carbon matrix. Figure 4 shows the data of the Raman study for the FeCoCu/C synthesized at different temperatures.

Direct comparison between the spectra showed that an increase in the nanocomposite synthesis temperature increases the intensity of the G band relative to that of the D band (Table 1). This fact indicates an increase in the ordering degree and the sizes of the crystallites in the graphite-like part of the matrix. In the meantime the high intensity and width of the bands near 1200–1300 and 1520–1540 cm^{-1} suggest there is a high relative content of amorphous carbon [21, 22]. An increase in the nanocomposite synthesis temperature reduces the content of amorphous carbon as can be seen from a decrease in the I_D/I_G and $I_{D'}/I_G$ intensity ratios. The low intensities of the 2D bands suggest the presence of at least two carbon phases,

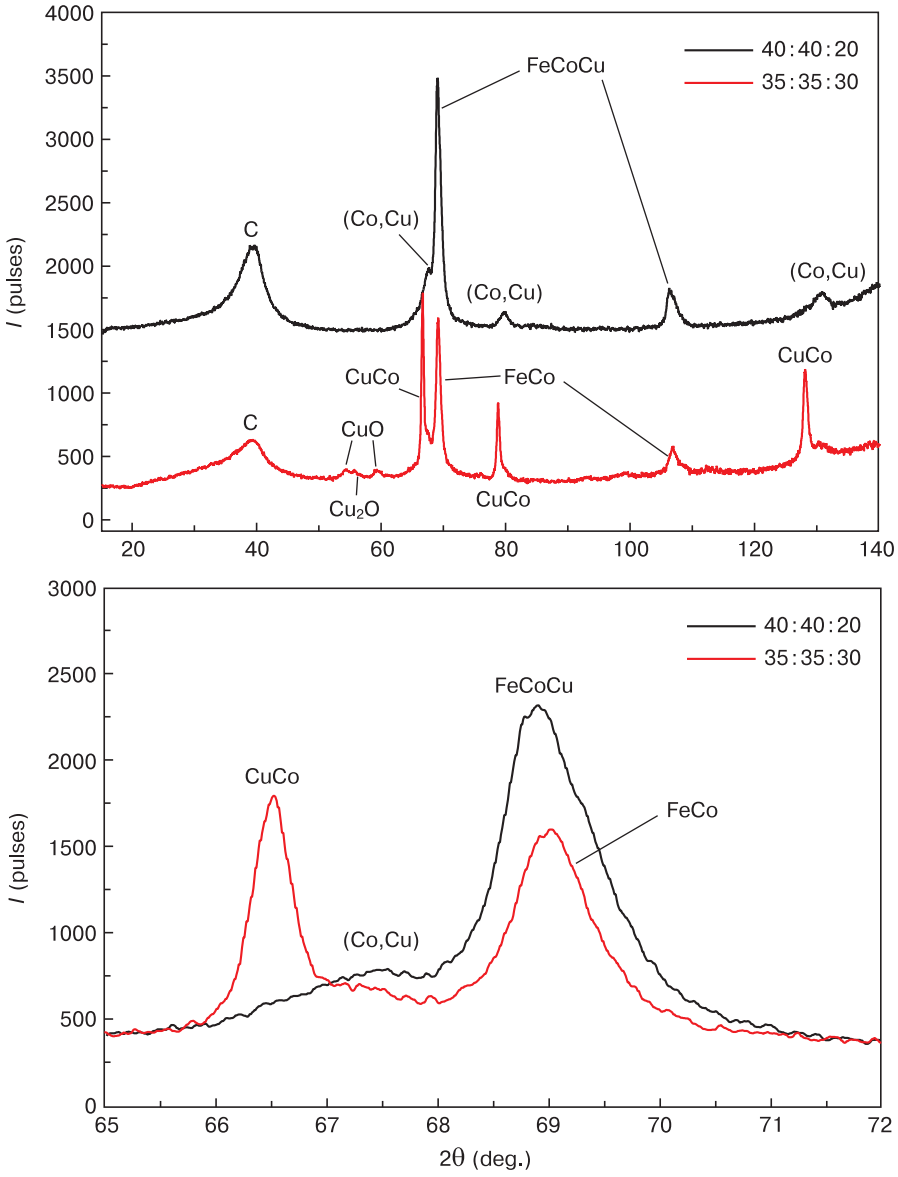

Figure 3. X-ray diffraction patterns of FeCoCu/C nanocomposites with different content ratios of metals

i.e., nanocrystalline graphite and amorphous graphite. An increase in the nanocomposite synthesis temperature reduces the I_{2D}/I_G intensity ratio which fact may indicate an increase in the number of layers in the graphite crystallites by analogy, for example, with an increase in the number of layers in graphene.

On the other hand, an increase in the relative content of copper in the nanocomposite slightly reduces the size of L_a, with the degree of amorphization increasing also. This is in a good agreement with the X-ray phase analysis data which also showed a decrease in the intensity and an increase in the width of the d_{002} peak.

Thus, analysis of the Raman spectra of the FeCoCu/C metal-carbon composites showed that the carbon matrix of the materials is a mixture of graphite nanocrystallites and amorphous graphite clusters and that an increase in the nanocomposite synthesis temperature increases the cluster sizes of the crystalline fraction in the microstructure of the carbon matrix. An increase in the Cu content in the nanocomposites hinders the structural ordering in the carbon matrix by reducing the solubility of carbon in the Fe-containing particles.

As was shown above for the example of nanocomposites with Ni or Al addition, the structural changes in the nanocomposite matrix and the changes in the size and composition of the nanoparticles or the relative content of copper in the precursor caused by an increase in the nanocomposire synthesis temperature entail tangible changes in the electromagnetic properties of the materials. We showed that the nanocomposites synthesized

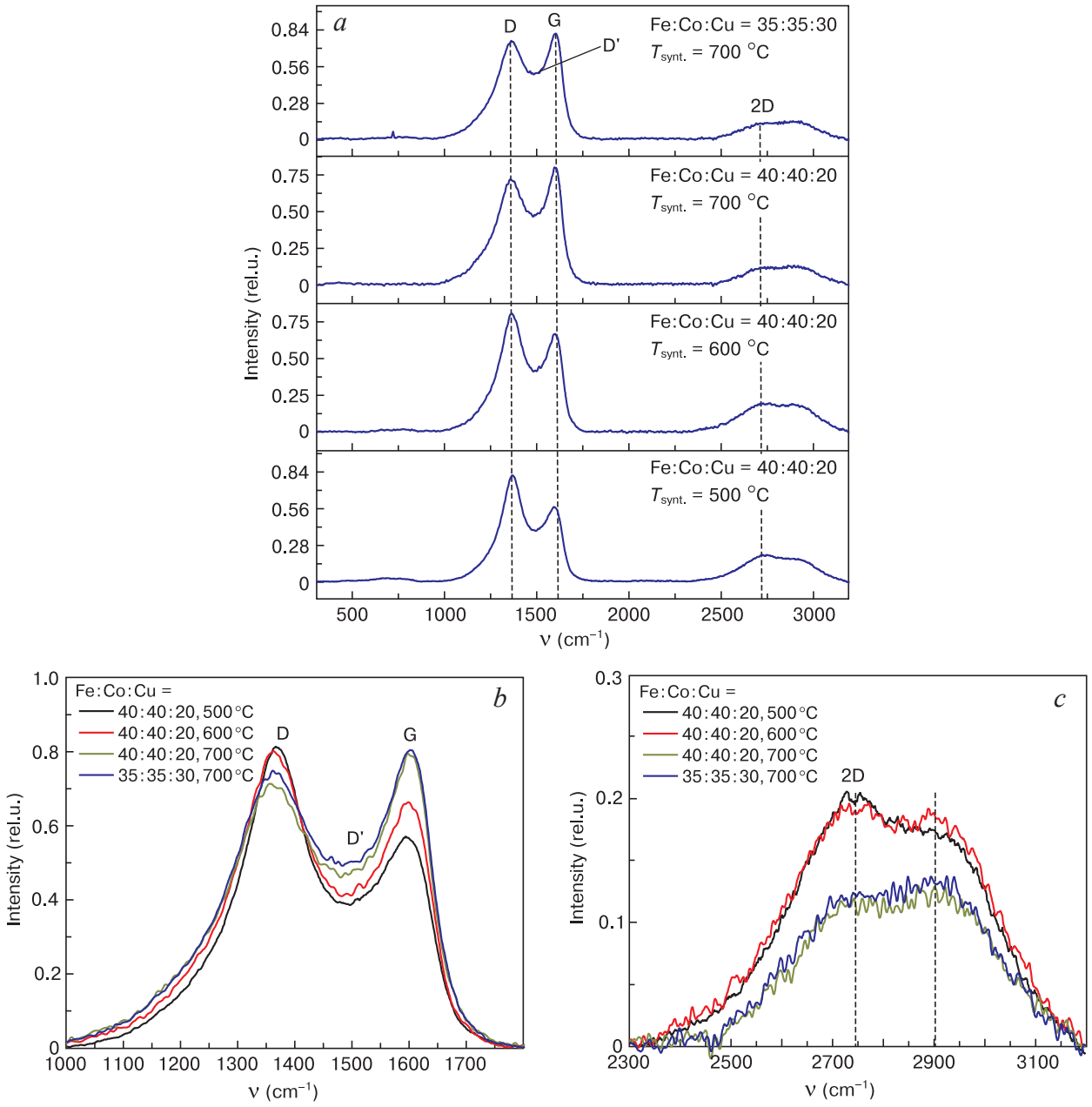

Figure 4. Raman spectra of FeCoCu/C nanocomposites synthesized at different temperatures and with different content ratios of metals: (*a*) survey spectra, normalized spectra of the regions of bands, (*b*) D and G, (*c*) 2D

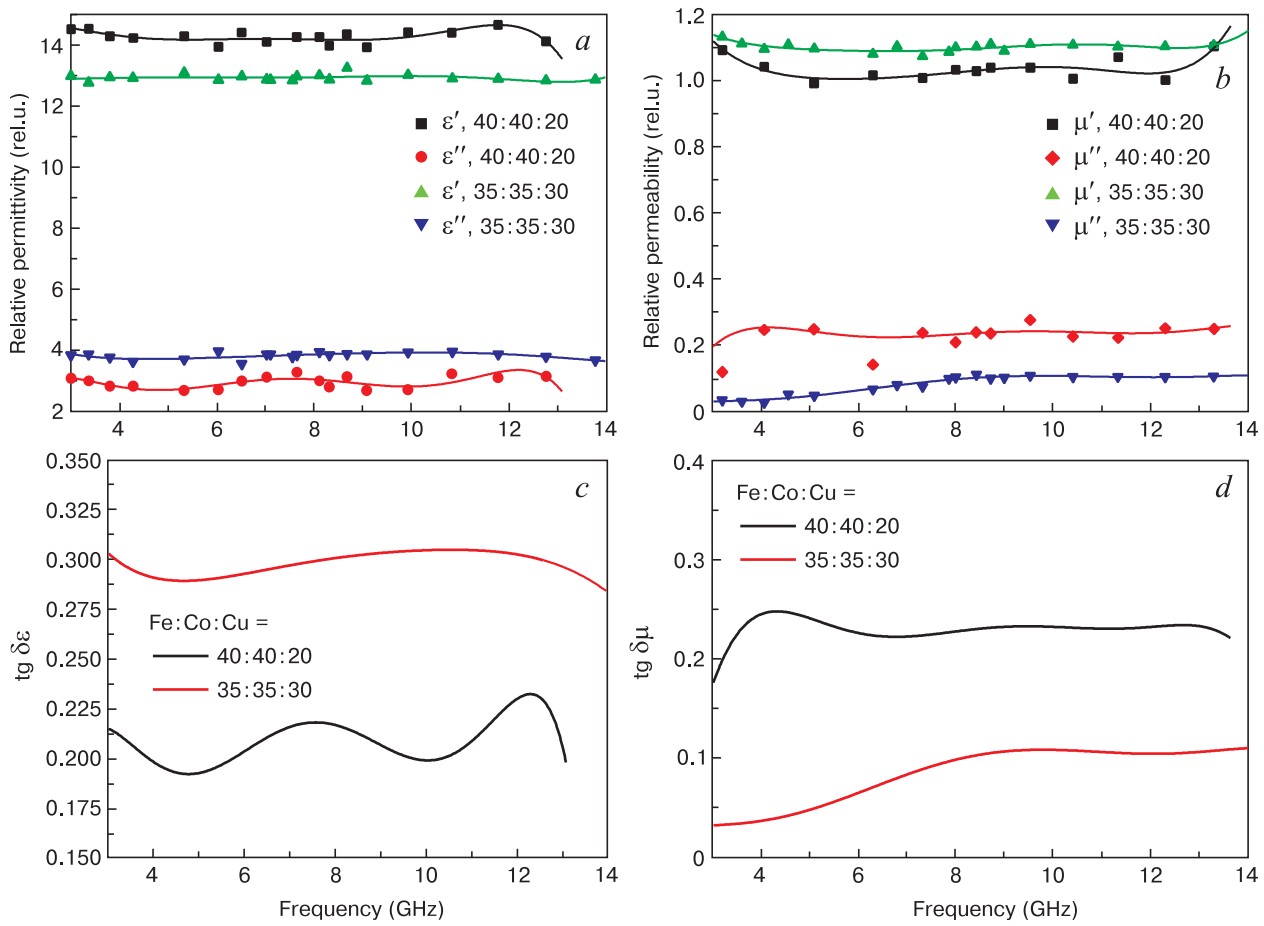

Figure 5. Frequency dependencies of relative (*a*) permittivity, (*b*) permeability, (*c*) dielectric and (*d*) magnetic loss tangents as a function of metal percentage in precursor

at T = 700 °C are the most promising ones, and we will therefore analyze the properties of FeCoCu/C system materials synthesized at 700 °C, with different metal content ratios.

Data on the effect of the metal content ratio on the dielectric and magnetic properties of the nanocomposites in microwave fields are presented in Fig. 5.

Analysis of the relative permittivity of the two selected FeCoCu alloy compositions showed that the real part of the permittivity of the nanocomposite having the Fe:Co:Cu = 40:40:20 metal content ratio is 14.5 at 3–14 GHz against 13.0 for the FeCoCu/C nanocomposite having the Fe:Co:Cu = 35:35:30 metal content ratio. The imaginary part of the permittivity of the nanocomposite having the Fe:Co:Cu = 40:40:20 metal content ratio is 3.0 at 3–14 GHz against ε”= 4.0 for the nanocomposite having the Fe:Co:Cu = 35:35:30 metal content ratio.

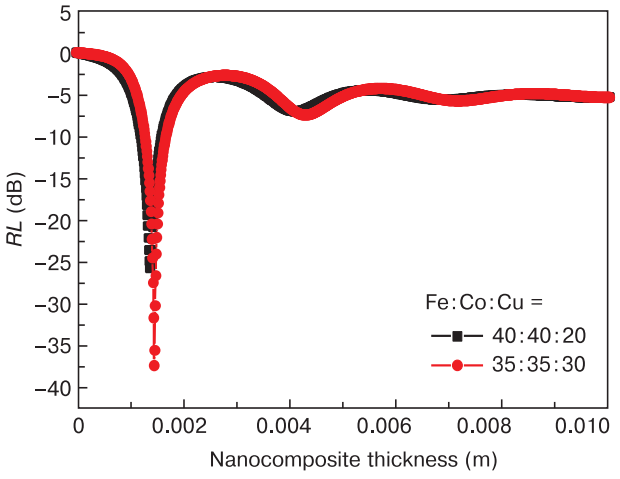

Figure 6. Absorber layer thickness optimization

An increase in the relative copper content in the nanocomposite reduces the magnetic loss tangent but increases the dielectric loss tangent. The decrease in the magnetic loss tangent is accounted for by a decrease in the imaginary part of the relative permeability which is in turn caused by a decrease in the general magnetization of the alloy. However the imaginary part of the relative permittivity increases, on the one hand, due to a more amorphous carbon matrix and, on the other hand, because of the formation of graphene-like carbon structures as indicated by Raman spectroscopy data. In the meantime the real part of the relative permittivity decreases, probably, because of an increase in the electrical conductivity of the nanocomposite due to the formation of copper-based alloy nanoparticles.

By way of comparison we present relative permittivity data for the FeCo/C nanocomposite [23]. The real relative

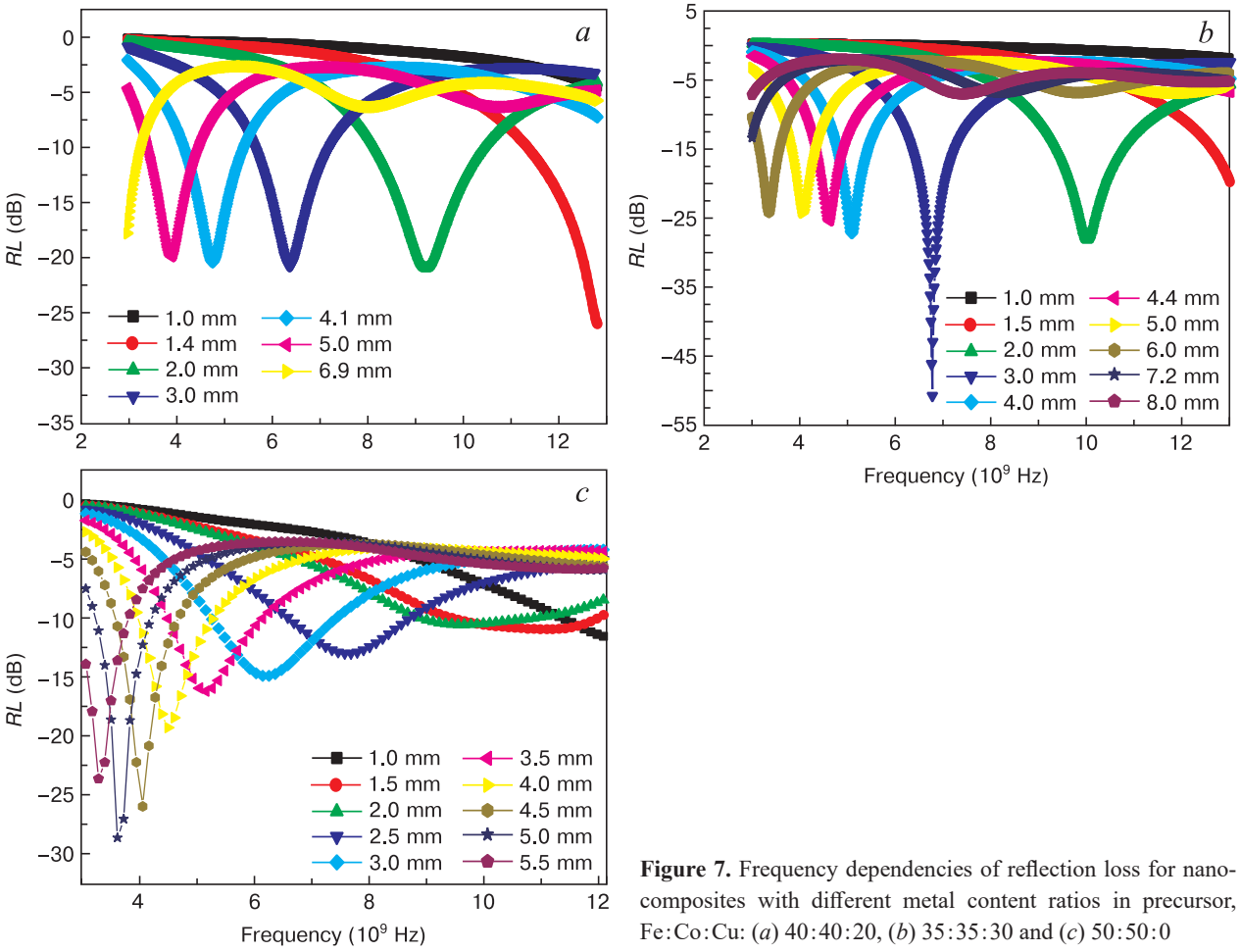

Figure 7. Frequency dependencies of reflection loss for nanocomposites with different metal content ratios in precursor, Fe:Co:Cu: (*a*) 40:40:20, (*b*) 35:35:30 and (*c*) 50:50:0

permittivity is ε′ = 12.5 for 2 GHz and decreases abruptly to ε′ = 3.0 for 18 GHz, whereas the imaginary relative permittivity is ε″ = 3.7 for 2 GHz and decreases to ε″ = 1.2 for 18 GHz. These data on the relative permittivity for the FeCoCu/C and FeCo/C nanocomposites suggest a great effect of Cu on the properties of the carbon matrix.

Figure 5 *b* illustrates the relative permeability of the FeCoCu/C nanocomposites having the Fe:Co:Cu = 35:35:30 and Fe:Co:Cu = 40:40:20 metal content ratios and synthesized at 700 °C. The real part of the relative permeability of the nanocomposite having the Fe:Co:Cu = 35:35:30 metal content ratio is 1.13 and remains constant in the 2–14 GHz range, while that of the nanocomposite having the Fe:Co:Cu = 40:40:20 metal content ratio is 1.02 and remains constant in the 4–12 GHz range. By way of comparison we present data on the real part of the relative permeability of the FeCo/C nanocomposite, which varies from 2.75 at 2 GHz to 1.5 at 18 GHz, and the imaginary part of the relative permeability of this nanocomposite, which varies in a stepwise manner from 1.0 at 2 GHz to 0.3 at 18 GHz. The ability of materials to absorb microwave radiation is characterized by the imaginary parts of their relative permittivity and permeability, whereas the ability to reflect microwave radiation is characterized by their real parts, provided the impedances of the ambient media and the surface layer of the active material are matched. Microporous composite materials satisfy these conditions to a sufficient extent in gas media, e.g. in the atmosphere. The μ′ and ε′ parameters are related to electromagnetic radiation energy transfer and the μ″ and ε″ ones, to energy loss or scatter in materials due to conductivity, resonance and relaxation mechanisms [24].

Calculations showed that the optimum thickness of FeCoCu/C nanocomposite based absorber layers is greater for specimens with a higher copper content (Fig. 6).

Analysis of the results shows that, taking into account the maximum magnetic loss, the optimum absorber layer thickness varies but slightly (from 1.4 to 1.5 mm) but the reflection index RL decreases significantly, from –26 to –38 dB.

Calculated data on the reflection loss for different absorber layer thicknesses are shown in Fig. 7.

4. Conclusion

Analysis showed that the FeCoCu/C nanocomposites are of interest since their reflection loss is between –20 and –32 dB (Fe:Co:Cu = 40:40:20) and between –25 and –52 dB (Fe:Co:Cu = 35:35:30) at 3–13 GHz. These values correspond to the reflection value of 0.9–0.97 and 0.944–0.997 rel.u. respectively and are higher than those for the FeCo/C nanocomposite (Fig. 7 *c*).

An increase in the nanocomposite layer thickness causes a shift of the reflection maximum towards lower frequencies because of resonance phenomena related to the thickness of the material. The magnitude of this shift decreases with an increase in the relative copper content in the nanocomposite. For a 3 mm layer of the nanocomposite having the Fe:Co:Cu = 35:35:30 metal content ratio, the abovementioned shift is 6.7 GHz (from 13.4 to 6.7 GHz), while for the FeCoCu/C nanocomposite having the Fe:Co:Cu = 40:40:20 metal content ratio this shift is 7.4 GHz (from 13.8 to 6.4 GHz). The nanocomposite having the Fe:Co:Cu = 35:35:30 metal content ratio has the lowest reflection value and should therefore be given preference.

Thus, by and large the FeCoCu/C nanocomposites in the frequency range studied in this experiment are the most efficient at the Fe:Co:Cu = 35:35:30 metal content ratio and hence are more promising, e.g. in comparison with the FeCo/C nanocomposites.

References

1. Lu A.-H., Salabas E.L., Schüth F. Magnetic nanoparticles: synthesis, protection, functionalization, and application. *Angewandte Chemie International Edition*. 2007; 46(8): 1222–1244. https://doi.org/10.1002/anie.200602866
2. Gubin S.P., Spichkin Y.I., Yurkov G.Yu., Tishin A.M. Nanomaterial for high-density magnetic data storage. *Russian Journal of Inorganic Chemistry*. 2002; 47(1): S32–S67.
3. Xu Y.H., Bai J., Wang J.-P. High-magnetic-moment multifunctional nanoparticles for nanomedicine applications. *Journal of Magnetism and Magnetic Materials*. 2007; 311(1): 131–134. https://doi.org/10.1016/j.jmmm.2006.11.174
4. Khadzhiev S.N., Kulikova M.V., Ivantsov M.I., Zemtsov L.M., Karpacheva G.P., Muratov D.G., Bondarenko G.N., Oknina N.V. Fischer-Tropsch synthesis in the presence of nanosized iron-polymer catalysts in a fixed-bed reactor. *Petroleum Chemistry*. 2016; 56: 522–528. https://doi.org/10.1134/S0965544116060049
5. Qiu F., Dai Y., Li Li, Xu Ch., Huang Y., Chen Ch., Wang Y., Jiao L., Yuan H. Synthesis of Cu@FeCo core-shellnanoparticles for the catalytic hydrolysis of ammonia borane. *International Jornal of Hydrogen Energy*. 2014; 39(1): 436–441.
6. Xu M.H., Zhong W., Qi X.S., Au C.T., Deng Y., Du Y.W. Highly stable Fe-Ni alloy nanoparticles encapsulated in carbon nanotubes: Synthesis, structure and magnetic properties. *Journal of Alloys and Compounds*. 2010; 495(1): 200–204. https://doi.org/10.1016/j.jallcom.2010.01.121
7. Bahgat M., Paek M.-K., Pak J.-J. Comparative synthesize of nanocrystalline Fe-Ni and Fe-Ni-Co alloys during hydrogen reduction of $Ni_xCo_{1-x}Fe_2O_4$. *Journal of Alloys and Compounds*. 2008; 466(1-2): 59–66. https://doi.org/10.1016/j.jallcom.2008.01.147
8. Azizi A., Yoozbashizadeh H., Sadrnezhaad S.K. Effect of hydrogen reduction on microstructure and magnetic properties of mechanochemically synthesized Fe-16.5Ni-16.5Co nano-powder. *Journal of Magnetism and Magnetic Materials.* 2009; 321(18): 2729–2732. https://doi.org/10.1016/j.jmmm.2009.03.085
9. Betancourt-Cantera L.G., Sánchez-De Jesús F., Bolarín-Miró A.M., Gallegos-Melgar A., Mayen J., Betancourt-Cantera J.A..Structural analysis and magnetic characterization of ternary alloys (Co–Fe–Ni) synthesized by mechanical alloying. *Journal of Materials Research and Technology.* 2020; 9(6): 14969–14978. https://doi.org/10.1016/j.jmrt.2020.10.068
10. Dalavi S.B., Theerthagiri J., Raja M.M., Panda R.N. Synthesis, characterization and magnetic properties of nanocrystalline $Fe_xNi_{80-x}Co_{20}$ ternary alloys. *Journal of Magnetism and Magnetic Materials*. 2013; 344: 30–34. https://doi.org/10.1016/j.jmmm.2013.05.026
11. Prasad N.Kr., Kumar V. Microstructure and magnetic properties of equiatomic FeNiCo alloy synthesized by mechanical alloying. *Journal of Materials Science: Materials in Electronics.* 2015; 26(12): 10109–10118. https://doi.org/10.1007/s10854-015-3695-7
12. Zehani K., Bez R., Boutahar A., Hlil E.K., Lassri H., Moscovici J., Mliki N., Bessais L. Structural, magnetic, and electronic properties of high moment FeCo nanoparticlesJ. *Journal of Alloys and Compounds*. 2014; 591: 58–64. https://doi.org/10.1016/j.jallcom.2013.11.208
13. Yang Y., Xu C., Xia Y., Wang T., Li F. Synthesis and microwave absorption properties of FECO nanoplates. *Journal of Alloys and Compounds*. 2010; 493(1-2): 549–552. https://doi.org/10.1016/j.jallcom.2009.12.153
14. Liu X.G., Ou Z.Q., Geng D.Y., Han Z., Jiang J.J., Liu W., Zhang Z.D. Influence of a graphite shell on the thermal and electromagnetic characteristics of FeNi nanoparticles. *Carbon.* 2010; 48(3): 891–897. https://doi.org/10.1016/j.carbon.2009.11.011
15. Li X., Takahashi S. Synthesis and magnetic properties of Fe–Co–Ni nanoparticles by hydrogen plasma-metal reaction. *Journal of Magnetism and Magnetic Materials*. 2000; 214(3): 195–203. https://doi.org/10.1016/S0304-8853(00)00081-0
16. Muratov D.G., Kozhitov L.V., Kazaryan T.M., Vasil'ev A.A., Popkova A.V., Korovin E.Yu. Synthesis and electromagnetic properties of FeCoNi/C nanocomposites based on polyvinyl alcohol. *Russian Microelectronics*. 2021; 50(8): 657–664. https://doi.org/10.1134/S1063739721080072
17. Muratov D.G., Kozhitov L.V., Korovushkin V.V., Korovin E.Yu., Popkova A.V., Novotortsev V.M. Synthesis, structure and electromagnetic properties of nanocomposites with threecomponent FeCoNi nanoparticles. *Russian Physics Journal*. 2019; 61(10): 1788–1797. https://doi.org/10.1007/s11182-019-01602-5
18. Muratov D.G., Kozhitov L.V., Yakushko E.V., Vasilev A.A., Popkova A.V., Tarala V.A., Korovin E.Yu. Synthesis, structure and electromagnetic properties of FeCoAl/C nanocomposites. *Modern Electronic Materials*. 2021; 7(3): 99–108. https://doi.org/10.3897/j.moem.7.3.77105
19. Mondal B.N., Basumallick A., Nath D.N., Cnattopaahyuy P.P. Phase evolution and magnetic, behavior of Cu-Ni-Co-Fe quaternary alloys synthesized by ball milling. *Material Chemistry and Physics.* 2009; 116(2): 358–362. https://doi.org/10.1016/j.matchemphys.2009.03.036

20. Vasilev A.A., Dzidziguri E.L., Efimov M.N., Muratov D.G., Karpacheva G.P. Formation of metal-carbon nanocomposites based on Cu-Fe alloy nanoparticles and carbonized polyacrylonitrile. *Fizika i khimiya obrabotki materialov = Physics and Chemistry of Materials Treatment.* 2021; (1): 58–66. (In Russ.). https://doi.org/10.30791/0015-3214-2021-1-58-66
21. Ferrari A.C., Robertson J. Interpretation of Raman spectra of disordered and amorphous carbon. *Physical Review B.* 2000; 61(20): 14095–14107. https://doi.org/10.1103/physrevb.61.14095
22. Ferrari A.C. Raman spectroscopy of graphene and graphite: Disorder, electron-phonon coupling, doping and nonadiabatic effects. *Solid State Communications.* 2007; 143(1-2): 47–57. https://doi.org/10.1016/j.ssc.2007.03.052
23. Afghahi S.S., Shokuhfar A. Two stepsinthesis, electromagnetic and microwave absorbing properties of FeCo@C core-shell nanostructure. *Journal of Magnetism and Magnetic Materials*. 2014; 370: 37–44. https://doi.org/10.1016/j.jmmm.2014.06.040
24. Rodionov V.V. Mechanisms of interaction of microwave radiation with nanostructured carbon-containing materials. Diss. Cand. Sci. (Phys.-Mat.). Kursk; 2015. 169 p. (In Russ.)